Spring Modeling of Suspension-Line Elasticity During the Parachute Unfurling Process," TN D-6671, 1972, NASA.

[4] Huckins, E. K., III, "A New Technique for Predicting the Snatch Force Generated During Lines-First Deployment of an Aerodynamic Decelerator," *Journal of Spacecraft and Rockets*, Vol. 8, No. 3, March 1971, pp. 298–299.

[5] Poole, L. R., "Numerical Solution of Equations Governing Longitudinal Suspension-Line Wave Motion During the Parachute Unfurling Process," M.S. thesis, May 1973, George Washington Univ., Washington, D.C.

[6] Bendura, R. J., Huckins, E. K., III, and Coltrane, L. C., "Performance of a 19.7-Meter-Diameter Disk-Gap-Band Parachute in a Simulated Martian Environment," TM X-1499, 1968, NASA.

[7] Dickinson, D., Schlemmer, J., Hicks, F., Michel, F., and Moog, R. D., "Balloon-Launched Decelerator Test Program Post-Flight Test Report, BLDT Vehicle AV-4," CR-112179, 1972, NASA.

JANUARY 1974 AIAA JOURNAL VOL. 12, NO. 1

# Unsteady Aerodynamic Response of a Two-Dimensional Airfoil at High Reduced Frequency

G. L. COMMERFORD* AND F. O. CARTA†
*United Aircraft Research Laboratories, East Hartford, Conn.*

**An experimental technique is described which corroborates the predictions of several new analyses of the unsteady response of an airfoil to high frequency flow fluctuations. The periodically fluctuating flowfield was produced by the natural shedding of vortices from a transverse cylinder to yield a reduced frequency of 3.9 based on airfoil semichord. Unsteady pressure measurements were made on an instrumented airfoil mounted downstream and above the turbulent wake of the cylinder. These unsteady pressures were found to be in good agreement with current compressible theories and show a chordwise variation of pressure phase angle which is not predicted by the incompressible analysis of Sears. Large reductions of the unsteady lift and phase angle were also observed for large airfoil incidence angles.**

## Nomenclature

| | |
|---|---|
| $a$ | = speed of sound |
| $b$ | = airfoil semichord |
| $C_L$, $C_M$ | = lift and moment coefficients |
| $C(k)$, $S(k)$, $T(k)$ | = unsteady aerodynamic functions |
| $f$ | = frequency |
| $k$ | = reduced frequency, $b\omega/U$ |
| $M$ | = Mach number, $U/a$ |
| $q$ | = dynamic pressure, $\rho U^2/2$ |
| $S^*(k)$ | = modified unsteady lift function |
| $u, v$ | = horizontal and vertical velocity perturbations |
| $U$ | = freestream velocity |
| $y$ | = vertical coordinate |
| $\alpha$ | = angle of attack |
| $\Gamma$ | = vortex strength |
| $\Delta L$ | = incremental lift |
| $\Delta p$ | = differential pressure |
| $\lambda$ | = wavelength |
| $\rho$ | = density |
| $\phi$ | = phase angle |
| $\omega$ | = frequency |

*Subscripts*

| | |
|---|---|
| $o$ | = amplitude |
| $v$ | = vertical |
| $H$ | = horizontal |
| $R$ | = real |
| $I$ | = imaginary |
| $S$ | = quasi-steady |

*Superscripts*

| | |
|---|---|
| * | = nondimensional coordinate |
| ¯ | = time-independent amplitude |

Presented as Paper 73-309 at the AIAA Dynamics Specialists Conference, Williamsburg, Va., March 19–20, 1973; received April 25, 1973; revision received August 24, 1973. This work was done in support of the Pratt & Whitney Aircraft Division of United Aircraft Corporation under NASA Contract NASW-1908, "Aerodynamic Broadband Noise Mechanisms Applicable to Axial Compressors."

Index categories: Nonsteady Aerodynamics; Aeroelasticity and Hydroelasticity.

* Formerly Research Engineer, Aeroelastics Group; presently Member of Technical Staff, Space Division, Rockwell International. Member AIAA.

† Supervisor, Aeroelastics Group. Associate Fellow AIAA.

## Introduction

IN computing the time-dependent forces and moments acting on an aerodynamic body, both the aeroelastician and the acoustician must necessarily consider an unsteady flowfield. This is because the physical processes in both cases involve relative motions at high frequency between the aerodynamic body and the airstream. Thus, an unsteady wake is produced which has an influence on the aerodynamic body and which is dependent on both time and distance. In general, the most important direct effects of unsteadiness are 1) phase differences between the aerodynamic forces and the motion producing them, and 2) an attenuation of the lift vector.

The unsteady aerodynamic theory associated with the flutter problem was derived in 1935 by Theodorsen.[1] He found that the unsteady lift or moment on an airfoil oscillating in both pitching and plunging could be expressed as functions of the respective quasi-steady lift (lift neglecting the influence of wake vortices on the flow) or moment, and a complex function, $C(k)$, known appropriately as the Theodorsen function. Sears[2] solved the similar problem of a stationary airfoil passing through a sinusoidally varying transverse gust. He found that the unsteady lift was equal to the steady lift at the effective gust angle of attack multiplied by a complex function $S(k)$, known as the Sears function.

The functions $C(k)$ and $S(k)$ are not significantly different at low reduced frequencies ($k < 0.3$) (cf. Refs. 3 and 4). However, as the reduced frequency becomes large ($k > 0.6$) the differences

between these two functions increase. The frequencies of interest in the acoustics problem, where Sears' theory is most often applied, correspond to disturbance wavelengths on the order of one airfoil chord length, which is equivalent to $k \approx \pi$ (because $k = b\omega/U = 2\pi b/\lambda$). Furthermore, there are two surprising results from Sears' theory that contradict intuition. First, the fluctuating lift "acts at all times at the quarter chord point of the airfoil" which Sears refers to in Ref. 2 as a "remarkable result." Second, the chordwise pressure distribution does not exhibit any variation in phase angle and hence there can be no pressure wave propagating along the airfoil chord, regardless of the frequency.

Another facet of this problem which has troubled theoreticians has been the necessity to use the incompressible Sears theory on a number of distinctly compressible problems. Typical of these problems are: 1) rotor blades passing through the wakes of stator blades in turbomachinery, 2) helicopter rotor blades encountering the tip vortices from preceding blades, and 3) aircraft flying through blast waves. Fortunately several analytical studies have appeared in recent years[5-8] which treat the complexities of three-dimensionality and compressibility in the unsteady problem. However, none of these new theories has been verified by direct experimentation, largely because of the inherent difficulties associated with experiments in this type of flowfield.

There have been many attempts in the past to create a controlled fluctuating flowfield in a wind tunnel. An excellent bibliography of this subject is contained in Ref. 9. Some of the techniques which have been tried include: 1) pulsing jets of air transverse to the flowfield, 2) oscillating airfoils on the sidewalls upstream of the test section, 3) moving the floor and ceiling in the test section, and 4) moving a set of ramps on the tunnel floor and ceiling. All of these techniques suffer from the same problems which are encountered in trying to oscillate a model airfoil in a steady flowfield, namely: 1) a large amount of external energy is required to produce the motion, and 2) the upper reduced frequency capability is still considerably lower than $k \approx 3.0$ at which $S(k)$ is desired.

One object of the present study was to employ an experimental technique to produce fluctuating velocity fields appropriate for an examination of Sears' theory. To this end, use was made of the periodic nature of the flow in the wake of a cylinder. This periodic flow is caused by the alternate shedding of vortices from the top and bottom of the cylinder, and the ensuing wake pattern is known as a Kármán vortex street. A detailed presentation of the theory of the Kármán vortex street is given in Ref. 10. Additional experimental data on Kármán streets both at low and high Reynolds numbers are contained in Refs. 11–14. A further object was to make a limited number of measurements which could be compared directly with the results of Sears' theory.

## Description of Experiment

A 3-in. chord, 4-in. span, 5% thick, symmetrical, double circular arc airfoil was selected for this program. The schematic diagram of Fig. 1 shows single surface pressure transducers at the 10, 20, 30, 60 and 90% chord locations. Another set of transducers were located on the opposite surface of the airfoil. With the 3-in. chord and the freestream velocity prescribed ($M = 0.25$) the required perturbation frequency to achieve a disturbance wavelength of one chord was $f = \omega/2\pi = kU/2\pi b = U/2b = 1120$ Hz. The frequency at which vortices are shed from a cylinder is a known function of Reynolds number. For $Re < 300$ the shedding reduced frequency based on cylinder diameter is approximately constant at 1.25 (Ref. 12). Fung points out in Ref. 4 that when $Re > 300$ the vortex shedding from a cylinder is "irregular"; i.e., a predominant frequency may be easily determined but its amplitude is more or less random. If tests were run at $M = 0.25$ with $Re < 300$ prohibitively small vertical separation distances between the rows of shed vortices would result. It was decided to accept the flow irregularities associated with $Re > 300$ in the hope that the flowfield would

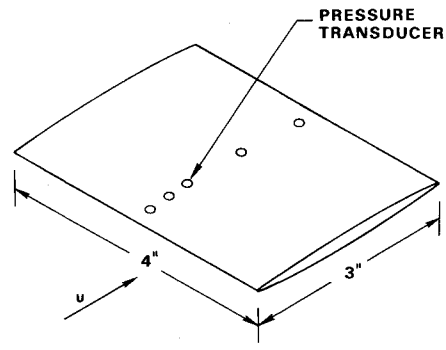


**Fig. 1 Schematic of model airfoil.**

be sufficiently periodic to yield meaningful results. The cylinder diameter required to produce the desired frequency at $M = 0.25$ was 0.54 in. This resulted in a Reynolds number of $0.82 \times 10^5$ which was well below $Re_{crit}$ of $4.5 \times 10^5$.

It is easily shown from the complex potential solution for a double row of vortices[15] that the vertical velocity fluctuation resulting from the presence of the vortices decays exponentially with the distance from the vortices. This has the form

$$v \approx \Gamma e^{-2\pi y/\lambda} = \Gamma e^{-\omega y/U} \tag{1}$$

In view of this behavior it was necessary to place the airfoil fairly close to the cylinder in order to obtain measurable perturbations. The vertical distance was limited by the exponential decay of the perturbation while the horizontal distance was limited by the fact that the periodic behavior of the flow disappears in the far wake at the Reynolds number of these tests. In using this type of flow to model the sinusoidal gust theories it was also necessary to examine the perturbation flowfield subject to the condition of zero vorticity. It can be shown directly[16] that for irrotational flow, the vertical velocity fluctuation must decay exponentially with distance in the same asymptotic manner as the vertical velocity fluctuation in the flow above the vortex street given in Eq. (1). It can also be shown that the horizontal fluctuations must decay in the same manner and that they must lead the vertical fluctuations by 90°.

In order to be precisely correct, it would be necessary to make measurements of the unsteady pressure on the airfoil and the unsteady velocity in the flowfield simultaneously. It did not appear likely that unsteady pressures over the airfoil would be unaffected by the presence of a hot-wire probe, so an alternate approach to this problem was used. The flowfield in the wake of the cylinder with the airfoil removed was surveyed using hot-wire anemometers. Simultaneously, measurements of the unsteady pressure fluctuation on the cylinder surface were made to establish the phase relationship between the upstream and downstream disturbances. Later in the experiment the hot-wire probe was removed and the unsteady airfoil pressures were measured with another simultaneous measurement of the cylinder pressure fluctuation. The relative phase angle measured earlier was then used to infer the "freestream" conditions approaching the airfoil. The cylinder pressure variation served only as a clock to relate the timewise variation in airfoil pressure to the timewise variation in the flowfield disturbances measured in a separate test. These two tests were run such that velocity repetition to within $\pm 1$ fps was achieved and the shedding frequency remained unchanged with and without the airfoil downstream of the cylinder.

All tests were conducted in the United Aircraft Research Lab. (UARL) 4-in. × 18-in. two-dimensional low-speed wind tunnel. This tunnel received air from a large pressurized plenum chamber. Flow passed through a series of three turbulence reducing screens and a rectangular bellmouth and exhausted to atmosphere.

The fluctuating flowfield was generated by mounting a cylinder in the forward portion of the test section. The cylinder contained

a $\frac{3}{16}$-in.-diam absolute pressure transducer. The transducer was located inside the cylinder with its active surface perpendicular to the axis of the cylinder. Since the magnitude of this pressure was not important it was only necessary to design the orifice leading to the transducer so that no phase shift in the pressure occurred as a result of the Helmholtz resonance of the cavity. This was accomplished by designing the cavity to yield a Helmholtz frequency several times higher than the shedding frequency.

Velocity fluctuations were obtained with two constant temperature hot-wire anemometers, each used in conjunction with a linearizer and a filter. This combination of instruments yielded outputs for both hot wires that were directly proportional to the velocity. The system frequency response was in excess of 20 kHz.

The airfoil was instrumented with ten miniature ($\frac{1}{8}$-in.-diam) pressure transducers. The transducers were used to obtain only the fluctuating (a.c. portion of output) pressures. Static pressure distributions at various angles of attack were obtained using conventional static pressure taps and a manometer board.

All other data taken during the course of this program were acquired and recorded using the UARL WISARD (Wide-Band System for Acquiring and Recording Data) data system discussed in Ref. 17. High frequency spectral analysis of the data was facilitated by recording at high FM tape speed and converting to digital format tapes later while playing back the FM tapes at low tape speed. All data were then processed with the UNIVAC 1108 digital computer.

## Experimental Results

### Steady-State Characteristics

Steady-state tests were conducted to obtain the lift coefficient, $C_L$, and the moment coefficient about the quarter chord, $C_M$. The steady-state stall defined by the departure of $C_L$ from linear and $C_M$ from zero occurred at $\alpha = 8°$. The maximum $C_L$ occurred at $\alpha = 12°$ and was equal to 0.8 (cf. Ref. 16).

### Flowfield Definition

Surveys of the wake using standard hot-wire anemometry techniques indicated that an acceptable position of the airfoil

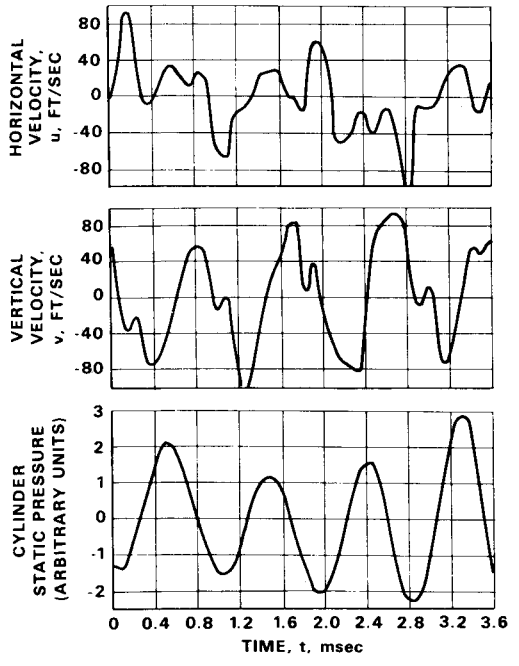


Fig. 2 Unsteady velocity fluctuations and cylinder pressure vs time.

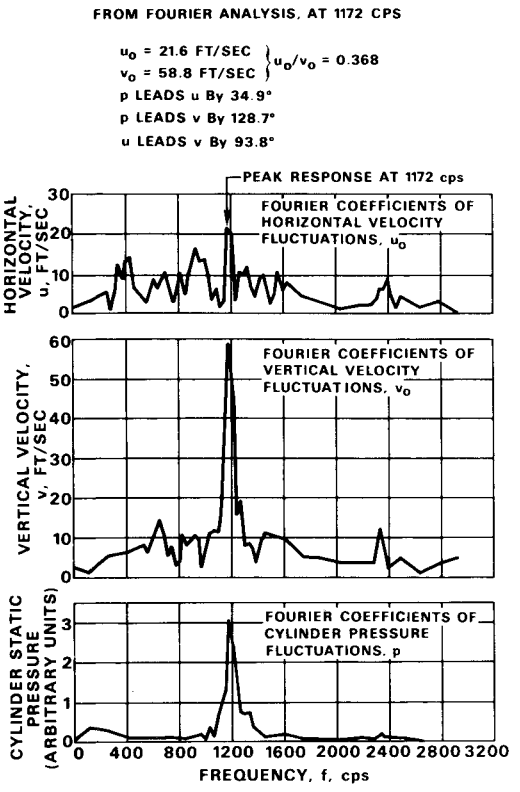


Fig. 3 Frequency response of velocity fluctuations and cylinder pressure.

L.E. relative to the center of the cylinder was 6.75 cylinder diameters (3.64 in.) downstream and 0.5 diam (0.27 in.) above the cylinder centerline. The horizontal and vertical velocity fluctuations together with the static pressure fluctuation on the cylinder are shown vs time in Fig. 2. A Fourier analysis of these signals showed a dominant peak at the shedding frequency (cf. Fig. 3). It is shown in the Appendix that the horizontal flow fluctuations do not contribute significantly to the unsteady lift for the actual test conditions. This fact was particularly true in these experiments because the amplitude $u_o$ was only about one-third as large as $v_o$. The vertical velocity fluctuations, on the other hand, show a sharp peak (four times as large as any other) at the shedding frequency. Since the vertical velocity is the most significant parameter, the "noise" in the signals does not restrict the usefulness of the results. The phase angles between each of these three signals taken in pairs were obtained by Fourier analysis. The horizontal velocity was observed to lead the vertical velocity by 90° as stated earlier.[16]

### Unsteady Pressure Distributions

In spite of the noisiness of the flow fluctuations, the periodicity of the individual pressure signals was well defined as can be seen from Fig. 4. Picture (a) shows the unsteady pressure at four chordwise locations on the pressure side of the airfoil to be approximately in phase. In picture (b) the cylinder pressure and the unsteady pressure at the 10% and 90% chord stations on the suction side of the airfoil are presented and a phase shift in the chordwise pressure distribution is apparent. This is discussed in greater detail below.

### Unsteady Measured Lift and Comparison with Theory

The final objective of this study was to make an experimental measurement of the unsteady lift. This was done by integrating the chordwise pressure difference distribution (extrapolated parabolically to the leading edge and to zero pressure at the trailing edge) at sequential instants of time. This yielded the lift coefficient vs time for each angle of attack. A typical plot for the

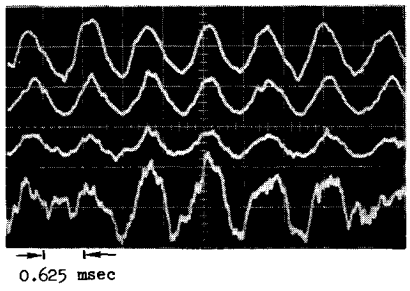


a) Pressures at 10%, 30%, 60% and 90% chord on pressure side of airfoil

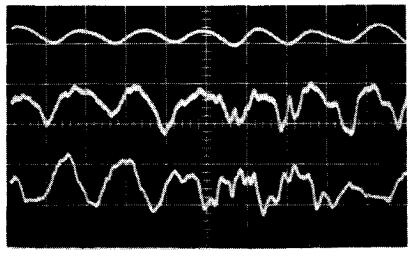

b) Cylinder pressure and pressures at 10% chord and 90% chord on suction side of airfoil

(All traces are from top to bottom with various scales to emphasize waveforms.)

**Fig. 4 Oscilloscope pictures of pressure signals.**

airfoil at zero degrees angle of attack is presented in Fig. 5. Despite the limited number of chordwise pressure transducers and the presence of background noise in the velocity fluctuations, the lift waveform is seen to be relatively noise free. Fourier analysis of this signal resulted in a spectrum which was virtually identical to that for the cylinder static pressure.

The conversion of the unsteady lift coefficient to a modified unsteady lift function vector in the phase plane suitable for comparing theory and experiment is discussed in the Appendix. Values of $S^*(k)$ were computed for the data obtained in the experiment, using the experimentally determined values of lift curve slope and effective angle of attack. Initially a comparison was made between these data and the original incompressible theory of Sears[3] as modified by the introduction of the Horlock correction.[18] This is shown in Fig. 6 in which only a portion of the phase plane spiral is included for clarity. The solid line is the original Sears theory for zero incidence. At each of the points representing values of $k$, a series of points denoting the changes in $S^*(k)$ due to the inclusion of horizontal velocity fluctuations at various nonzero incidence angles are appended. It can be seen that these horizontal flow fluctuations cause

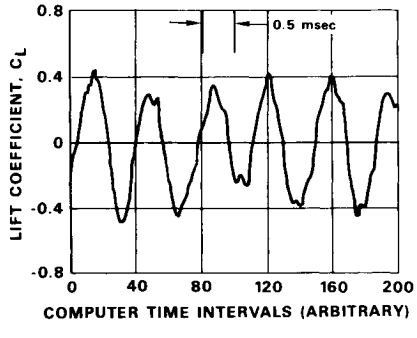


**Fig. 5 Lift coefficients vs time.**

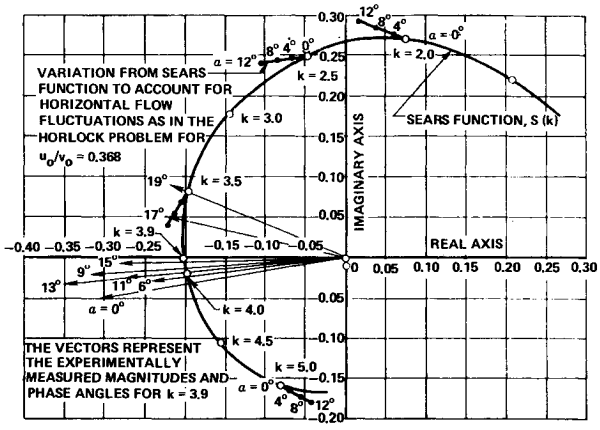


**Fig. 6 Phase plane with experimental results.**

an increase in both magnitude and phase lead angle of $S^*(k)$, although the over-all effect is small.

The experimental results for $k = 3.9$ [where the theoretical $S(k) = -0.201 + 0i$] are shown as individual vectors for each airfoil angle of attack. The value $k = 3.9$ is based on the mean freestream velocity at the airfoil. The experimental values of $S^*(k)$ for low angle of attack always exceed the theory in magnitude with roughly the same phase lead as the theory. These results are also shown in Fig. 7 vs angle of attack. The large decrease in phase angle for $\alpha > 13°$ is an indication of dynamic stall at an angle of attack much greater than the steady-state stall angle of $\alpha = 8°$. The small variation in the theoretical curve represents the change due to horizontal flow fluctuations at the various angles of attack.

Finally, we shall consider the chordwise variation of unsteady pressure on the airfoil in detail. An expression for the theoretical unsteady pressure at zero incidence angle for incompressible flow can be derived from the Sears formulation and is presented in Ref. 16. The result shows that the unsteady pressure is equal to the quasi-steady pressure times the Sears function, i.e., the phase angle of any point along the chord of the airfoil

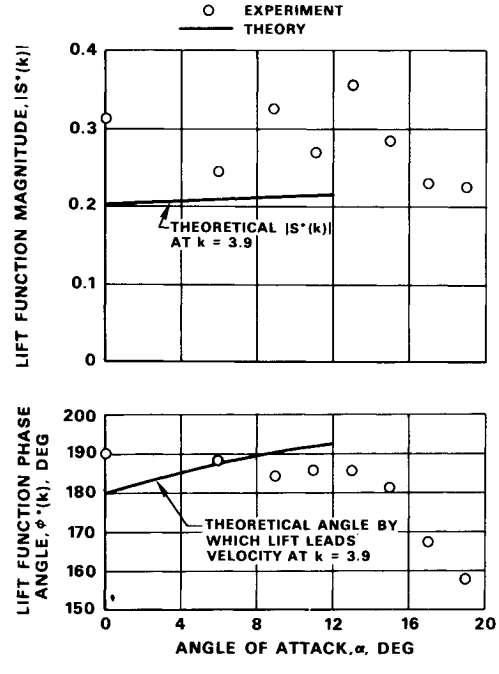


**Fig. 7 Unsteady lift magnitude and phase angle vs angle of attack.**

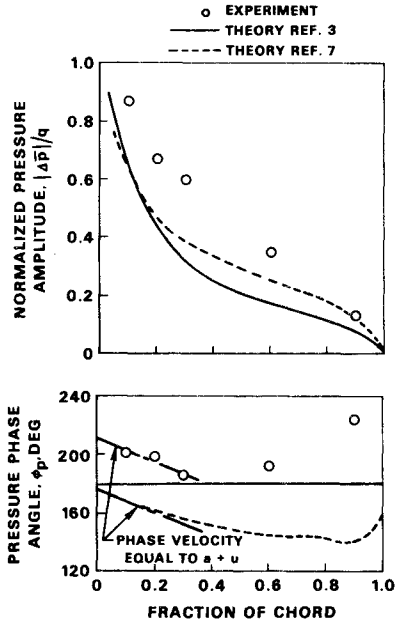


**Fig. 8 Comparison of chordwise pressure magnitude and phase angle with theory.**

relative to flow fluctuations at the midchord is constant and equal to the phase lead of the unsteady lift. The picture in Fig. 4b showed this was not the case in the experiment. Figure 8 shows the theoretical and experimental chordwise pressure distribution at $\alpha = 0$. The experimental magnitude is seen to exceed the theoretical prediction of Sears. The experimental phase angle decreases from the leading edge and then increases toward the trailing edge as opposed to the theory which predicts a constant pressure phase angle of 180° for $k = 3.9$. A chordwise variation in pressure phase angle can have significant consequences in many unsteady problems. For example, one would expect a variation in aerodynamic noise as a result of the chordwise phase variation of the pressure signal, and further one would expect an unsteady moment to be developed which was not predicted by Sears.

Although the freestream Mach number in this program was such that the test appears to be incompressible, it should be noted that the compressible reduced frequency parameter $kM/(1-M^2)^{1/2} = 0.82$. This compressible reduced frequency is well within the range where compressibility effects become important. The addition of compressibility effects to Sears' theory has been treated in Refs. 6–8. It is appropriate therefore to compare the test results to the compressible theory of Adamczyk[7] whose results are also shown in Fig. 8. Here it is seen that the pressure amplitude is in slightly better agreement with experiment than the incompressible Sears theory. Furthermore, the predicted pressure phase angle shows a variation over the chord which is in qualitative agreement with the experiment; i.e., although the magnitude does not agree, the local slopes are in good agreement, particularly at the leading and trailing edges. This is felt to be important because Adamczyk has shown that these slopes represent the propagation of energy aft from the leading edge at a velocity equal to the sum $a+U$, and forward from the trailing edge at a velocity equal to the difference $a-U$, where $U$ is the freestream velocity and $a$ is the speed of sound.

## Conclusions

1) A useful technique has been developed for making meaningful unsteady aerodynamic response measurements at high reduced frequencies.

2) The limited experimental results at $k = 3.9$ show greater unsteady lift magnitude than incompressible theory with generally similar phase angles relative to the fluctuating flow velocity.

3) The experimental chordwise pressure distribution indicates that a phase angle variation exists. This result is not predicted by incompressible theory but is found in compressible analyses.

4) The individual pressure distributions at each angle of attack all tended to zero at the trailing edge indicating that the Kutta condition was satisfied even at this high reduced frequency.

## Appendix: Unsteady Lift from Vertical and Horizontal Flow Fluctuations

In Ref. 3 Sears gives the unsteady lift resulting from a sinusoidal vertical gust as

$$\Delta L_v(k) = 2\pi\rho U b v S(k) = \Delta\bar{L}_v e^{i\omega t} \tag{2}$$

where $S(k)$ is the unsteady Sears function discussed in the Introduction. A similar expression has been obtained by Horlock,[18] where the unsteady lift resulting from a sinusoidal horizontal gust was shown to be

$$\Delta L_H(k) = 2\pi\rho U b u \alpha T(k) = \Delta\bar{L}_H e^{i\omega t} \tag{3}$$

where $T(k)$ is the unsteady Horlock function similar in character to that of Sears.

If the perturbation velocity in the vertical direction is written in the form

$$v = v_o e^{i\omega t} \tag{4}$$

then the horizontal perturbation velocity, with lead angle of $\pi/2$, is

$$u = u_o e^{i(\omega t + \pi/2)} = i u_o e^{i\omega t} \tag{5}$$

When Eqs. (2–5) are combined and simplified the total incremental lift due to both vertical and horizontal fluctuations can be written as

$$C_L(k) = C_{L_R} + iC_{L_I} = \frac{2\pi v_o}{U}\left[\left(S_R - \frac{u_o\alpha}{v_o}T_I\right) + i\left(S_I + \frac{u_o\alpha}{v_o}T_R\right)\right] \tag{6}$$

It is convenient at this point to define a modified unsteady lift function $S^*(k)$ equal to the bracketed terms in Eq. (6) such that

$$C_L(k) = (2\pi v_o/U)S^*(k) \tag{7}$$

The effect of the deviation of the experimental lift-curve slope from the theoretical value of $2\pi$ may now be included. The quantity $2\pi v_o/U$ is equivalent to the quasi-steady lift coefficient, $C_{L_S}$; i.e., the product of the theoretical lift-curve slope, $2\pi$, and the angle-of-attack amplitude, $v_o/U$. Hence, Eq. (7) may be rewritten as

$$S^*(k) = C_L(k)/C_{L_S} \tag{8}$$

in which the right-hand side represents the ratio of theoretical quantities. However, if the actual value of the experimental lift-curve slope ($dC_{L_S}/d\alpha = 5.14$ rad$^{-1}$) and the actual velocity ratio $v_o/U$ are used to replace $2\pi v_o/U$ then the denominator of Eq. (8) is the measured quasi-steady lift of the airfoil. If, further, the actual measured value of $C_L(k)$ is inserted into the numerator of Eq. (8) the resulting value of $S^*(k)$ is the experimentally measured unsteady lift function which is now in a suitable form for direct comparison with available theories.

## References

[1] Theodorsen, T., "General Theory of Aerodynamic Instability and the Mechanics of Flutter," Rept. 496, 1934, NACA.

[2] Sears, W. R., "Some Aspects of Non-Stationary Airfoil Theory and Its Practical Application," *Journal of the Aeronautical Sciences*, Vol. 8, 1941, pp. 104–108.

[3] Bisplinghoff, R. L., Ashley, H., and Halfman, R. L., *Aeroelasticity*, Addison-Wesley, Reading, Mass., 1955.

[4] Fung, Y. C., *An Introduction to the Theory of Aeroelasticity*, Wiley, New York, 1955.

[5] Filotas, L. T., "Response of an Infinite Wing to an Oblique Sinusoidal Gust," NASA SP-207, 1969, pp. 231–246.

[6] Graham, J. M. R., "Similarity Rules for Thin Aerofoils in Non-

Stationary Subsonic Flows," *Journal of Fluid Mechanics,* Vol. 43, 1970, p. 753.

[7] Adamczyk, J. J., "Passage of an Isolated Airfoil Through a Three-Dimensional Disturbance," Ph.D. thesis, May 1971, Univ. of Connecticut, Storrs, Conn.

[8] Adamczyk, J. J. and Brand, R. S., "Scattering of Sound by an Aerofoil of Finite Span in a Compressible Stream," *Journal of Sound and Vibrations,* Vol. 25, 1972, pp. 139–156.

[9] Gollnick, A., "The Generation of Periodic Gusts in a Supersonic Wind Tunnel," Rept. SP276, June 1969, MIT, Cambridge, Mass.

[10] Lamb, H., *Hydrodynamics.* 6th ed. Dover Publications, New York, 1945.

[11] Kovasznay, L. S. G., "Hot Wire Investigation of the Wake Behind Cylinders at Low Reynolds Numbers," *Proceedings of the Royal Society, London, Series A,* Vol. 198, 1949, pp. 174–190.

[12] Roshko, A., "On the Development of Turbulent Wakes from Vortex Streets," Rept. 1191, 1954, NACA.

[13] Bearman, P. W., "On Vortex Shedding from a Circular Cylinder in the Critical Reynolds Number Regime," *Journal of Fluid Mechanics,* Vol. 37, Pt. 3, 1969, pp. 577–585.

[14] Sallet, D. W., "On the Spacing of Kármán Vortices," *Transactions of the ASME: Journal of Applied Mechanics,* Vol. 36, No. 2, June 1969, pp. 370–372.

[15] Milne-Thomson, L. M., *Theoretical Hydrodynamics,* 4th ed., Macmillan Co., New York, 1960.

[16] Commerford, G. L. and Carta, F. O., "An Exploratory Investigation of the Unsteady Aerodynamic Response of a Two-Dimensional Airfoil at High Reduced Frequency," AIAA Paper 73-309, Williamsburg, Va., 1973.

[17] Ward, D. and Cohen, W., "Wide-Band System for Acquiring and Recording Data (WISARD)," Rept. H-076944-1, Oct. 1969, United Aircraft Research Labs., East Hartford, Conn.

[18] Horlock, J. H., "Fluctuating Lift Forces on Aerofoils Moving Through Transverse and Chordwise Gusts," *Transactions of the ASME: Journal of Basic Engineering,* Vol. 90, Ser. D, No. 4, Dec. 1968, pp. 494–500.